

The aryl hydrocarbon receptor (AHR) transcription factor regulates megakaryocytic polyploidization

Stephan Lindsey and Eleftherios T. Papoutsakis

Department of Chemical Engineering and Delaware Biotechnology Institute, University of Delaware, Newark, DE, USA

Summary

We propose that the aryl hydrocarbon receptor (AHR) is a novel transcriptional regulator of megakaryopoietic polyploidization. Functional evidence was obtained that AHR impacts *in vivo* megakaryocytic differentiation and maturation; compared to wild-type mice, *AHR*-null mice had lower platelet counts, fewer numbers of newly synthesized platelets, increased bleeding times and lower-ploidy megakaryocytes (Mks). *AHR* mRNA increased 3-6-fold during *ex vivo* megakaryocytic differentiation, but reduced or remained constant during parallel isogenic granulocytic or erythroid differentiation. We interrogated the role of AHR in megakaryopoiesis using a validated Mk model of megakaryopoiesis, the human megakaryoblastic leukaemia CHRF cell line. Upon CHRF Mk differentiation, *AHR* mRNA and protein levels increased, AHR protein shifted from the cytoplasm to the nucleus and AHR binding to its consensus DNA binding sequence increased. Protein and mRNA levels of the AHR transcriptional target *HES1* also increased. Mk differentiation of CHRF cells where *AHR* or *HES1* was knocked-down using RNAi resulted in lower ploidy distributions and cells that were incapable of reaching ploidy classes $\geq 16n$. *AHR* knockdown also resulted in increased DNA synthesis of lower ploidy cells, without impacting apoptosis. Together, these data support a role for *AHR* in Mk polyploidization and *in vivo* platelet function, and warrant further detailed investigations.

Keywords: megakaryocytopoiesis, thrombopoietin, cell biology, transcription factors, haematopoiesis.

Received 17 September 2010, accepted for publication 16 November 2010

Correspondence: Stephan Lindsey, PhD, Department of Chemical Engineering and Delaware Biotechnology Institute, University of Delaware, 15 Innovation Way, Newark, DE 19711, USA.
E-mail: slindsey@udel.edu

Well-known as a 'toxin sensor', the aryl hydrocarbon receptor (*AHR*) is a member of the Per-Arnt-Sim (PAS) family of basic helix-loop-helix transcription factor family, and is involved in the mechanism of action of various environmental toxins, presumably by altering cell cycle regulation (Ma & Whitlock, 1996). While *AHR* is highly conserved throughout evolution (even in organisms, such as *Caenorhabditis elegans*, that are insensitive to canonical AHR toxic ligands), an endogenous ligand and physiological role for AHR has, for the most part, eluded researchers (Nguyen & Bradfield, 2008). Despite lacking a clear endogenous ligand, AHR appears to play a role in the differentiation of many developmental pathways, including T-cells (Quintana *et al*, 2008), neurons (Akahoshi *et al*, 2006) and hepatocytes (Walisser *et al*, 2005). AHR antagonists have been shown to promote haematopoietic stem cell expansion and treatments with AHR agonists

demonstrate a key role of AHR in haematopoietic stem-cell biology (Singh *et al*, 2009; Boitano *et al*, 2010), supporting our hypothesis that AHR plays an important developmental role beyond toxicology, especially within the haematopoietic compartment. Although no platelet defects have been reported in *AHR*-null mice, these mice develop extramedullary haematopoiesis similar to *GATA1^{low}* mice (Schmidt *et al*, 1996; Vannucchi *et al*, 2002). Furthermore, the AHR signaling pathway regulates many several important regulators of megakaryopoiesis, including *NRF2*, a key activator of stress-responsive genes recently shown to compete with *NF-E2* during megakaryocytic (Mk) differentiation (Miao *et al*, 2005; Motohashi *et al*, 2010) and survivin (Kang & Altieri, 2006; Vargiolu *et al*, 2009). In addition, exposure to toxic waste containing known AHR ligands results in significantly higher platelet counts (Webb *et al*, 1987), and a 2001 study of

Vietnam veterans found that those exposed to high levels of 2,3,7,8-Tetrachlorodibenzodioxin (TCDD; an identified AHR ligand) had increased platelet counts proportional to the dose they had received (Michalek *et al*, 2001). While correlative, these studies offer the intriguing possibility that AHR modulates platelet production.

Other studies found that AHR ligands do not alter megakaryocyte (Mk) numbers or morphology, yet result in decreased platelet numbers (Weissberg & Zinkl, 1973), and that perinatal exposure to dioxin results in decreased platelet counts inversely proportional to the amount of dioxin exposure (Pluim *et al*, 1994; ten Tusscher *et al*, 2003). These contradictory findings suggest that either the effects of toxicological AHR ligands are context- and developmental stage-dependent, or that there is unknown cross-talk between AHR and other signaling pathways. They also highlight the artificial nature of toxicological ligands, and point to the need to identify endogenous ligands before the physiological role of AHR can be determined. Based on these observations, we chose to further investigate the role of AHR during Mk differentiation and maturation. The first goal of this study was to determine whether AHR expression supports the hypothesis that AHR plays a role in megakaryopoiesis. The second goal, using *AHR*-null mice, was to test if AHR affects *in vivo* platelet production and function. The third goal was to investigate whether RNAi-mediated reduction of *AHR* expression in CHRF cells [a human megakaryoblastic leukaemia cell line model of human Mk differentiation (Fuhrken *et al*, 2007)] results in decreased Mk polyploidization, possibly explaining any decreased platelet production.

Previous investigations employed a genome wide approach to identify genes upregulated during Mk differentiation of human CD34⁺ cells (Chen *et al*, 2007). During these microarray experiments, *AHR* expression increased two to threefold as megakaryopoiesis progressed, while parallel isogenic granulocytic cells demonstrated a twofold decrease in *AHR* expression. Increased *AHR* expression was Mk-specific, as expression was 4–7 higher in Mks than isogenic, cultured granulocytic (G) cells derived from the same CD34⁺ cultures.

Materials and methods

Differentiation of primary human cells

Cultures were initiated in T flasks with previously frozen CD34⁺ cells isolated from granulocyte colony-stimulating factor (G-CSF) mobilized human peripheral blood (enriched by magnetic bead isolation to greater than 95% purity by the Fred Hutchinson Cancer Research Center; Seattle, WA). All cytokines were purchased from Peprotech (Rocky Hill, NJ, USA) unless otherwise noted. Mk cultures were maintained at a concentration between 100 000 and 300 000 cells/ml and supplemented with 100 ng/ml thrombopoietin (Tpo) to

induce Mk differentiation as described (Giammona *et al*, 2006). Granulocytic cultures were maintained at a concentration between 30 000 and 300 000 cells/ml in human long-term media (HLTM) supplemented with 10 ng/ml interleukin (IL)-3, 10 ng/ml IL-6, 10 ng/ml G-CSF and 50 ng/ml stem cell factor (SCF) (Hevehan *et al*, 2000). Erythroid cultures were maintained at a concentration between 100 000 and 400 000 cells/ml in HLTM supplemented with 10 ng/ml IL-3, 10 ng/ml IL-6, 50 ng/ml SCF and 3 u/ml Erythropoietin [Cell Sciences (McAdams *et al*, 1998)].

CHRF differentiation. CHRF cells (Fuhrken *et al*, 2007) were maintained at 50 000–75 000 cells/ml and differentiated toward the Mk lineage with 10 ng/ml phorbol myristate acetate (PMA) in dimethyl sulfoxide (DMSO). At designated time-points, cells were washed twice with phosphate-buffered saline (PBS) and harvested using 1× cell dissociation buffer (PBS with 1 mmol/l EDTA). Adherent and non-adherent cell fractions were combined for all analyses.

Quantitative reverse transcription polymerase chain reaction (Q-RT-PCR)

Q-RT-PCR was performed using the High-Capacity cDNA Archive kit and Assays-on-Demand Taqman kit following the manufacturer's protocols (Applied Biosystems; Foster City, CA, USA), with slight modifications (Fuhrken *et al*, 2008a). The Applied Biosystems primer sets used were: Hs00169233_m1 (*AHR*), Hs00172878_m1 (*HES1*), Hs99999908_m1 (*GUSB β*) and Hs99999902_m1 (*RPLP0*). A serial dilution of a reference sample (an equal-mass mixture of all samples to be tested) was used to verify linearity of the assay and cycle threshold values were determined and converted to starting mass units (SMU) using iCycler software (Bio-Rad, Hercules, CA, USA).

Western blot analysis

For total cell lysates, cell pellets were lysed by boiling in 2× sodium dodecyl sulphate (SDS) sample buffer. Lysate proteins (20 μ g) were separated by SDS-polyacrylamide gel electrophoresis (SDS-PAGE) and transferred to nitrocellulose according to standard techniques. Western blots were serially probed with antibodies to AHR, HES1 and either beta-actin or glyceraldehyde-3-phosphate dehydrogenase (Santa Cruz Biotechnologies, Santa Cruz, CA, USA) as loading controls. Densitometry analysis was performed using ImageJ Software version 1.38 (NIH, Bethesda, MD, USA). Nuclear extract proteins were isolated from CHRF cells by the method of Dignam *et al* (1983) with protease inhibitors as described (Lindsey *et al*, 2007). Western blots for HDAC1 and FAK (Abcam, Cambridge, MA, USA) verified that there was no contamination between the fractions. In some experiments, CHRF cells were differentiated into Mks with 10 ng/ml PMA before nuclear-protein isolation.

Electromobility shift assay (EMSA)

EMSA analyses were carried out as described (Lindsey *et al*, 2005) using an EMSA kit (Panomics, Santa Clara, CA, USA) following manufacturer's instructions. The biotinylated probes used were based on published DNA recognition sequences (Denison *et al*, 1988) and designed to represent either an AHR consensus binding sequence (5'-GGGGATCGCGTGACAACC-3') or the region corresponding to the putative AHR binding site within the HES1 promoter (ACGAGCCGTTTCGCGTGCAGTCCCAG); putative AHR DNA recognition sites are underlined. Nuclear extracts used in these experiments were prepared as described. In each sample, nuclear extract proteins were incubated with biotinylated oligonucleotides; some samples were preincubated with unlabeled consensus binding sequence oligonucleotides to verify band specificity. Control samples were incubated with antibodies toward AHR or glutathione S-transferase (Santa Cruz Biotechnologies). Separation of bound and free probe was achieved by electrophoresis using a 6.0% non-denaturing polyacrylamide gel, and the protein-DNA complexes were transferred to a Biotodyne B nylon membrane (Pall, Port Washington, NY, USA). Protein-DNA complexes were detected using streptavidin-horseradish peroxidase and visualized after exposure to Hyperfilm enhanced chemiluminescence film (GE Healthcare Biosciences, Piscataway, NJ, USA). Densitometry analysis was performed on probe-specific region(s) and normalized to the amount of probe present in each sample using ImageJ software.

Chromatin Immunoprecipitation

CHRF cells were cultured with or without PMA for 7 d as described above. Cells for chromatin immunoprecipitation were incubated with formaldehyde prior to lysis, and lysates were sonicated to generate chromatin fragments with an average size of 200 kb as described (Lindsey *et al*, 2007). Lysates underwent immunoprecipitation with either antibodies toward AHR or Immunoglobulin G. Coprecipitated chromatin was analyzed by PCR for AHR-specific antibody coprecipitation of the HES1 gene promoter using the following primers: HES1 F – 5'-CTGTGGGAAAGAAAGTTTGGGAAG-3'; HES1 R – 5'-GCTCCGGATCCTGTGTGATCC-3'. For these experiments, input chromatin was used as a positive control and chromatin precipitated by Immunoglobulin G was used as a negative control. PCR products were analyzed by acrylamide gel electrophoresis.

Mice

AHR-null mice were previously generated and kindly provided by Dr. Christopher Bradfield (Schmidt *et al*, 1996). Mice homozygous (AHR^{-/-}) and heterozygous (AHR^{+/-}) for the null allele were generated by intercrossing AHR^{-/-} male mice with AHR^{+/-} female mice. These mice have been backcrossed

for 20 generations to the C57BL6/J background and wild-type (WT) mice are indistinguishable from littermate control mice. Therefore, age-matched WT C57BL6/J mice (Jackson Laboratory, Bar Harbor, ME, USA) serve as control mice for these studies. The current research compared only female mice, although we observed similar effects between male mice (data not shown).

Murine experiments

Bleeding time assays were performed as described (Jirouskova *et al*, 2007). Briefly, mice were anesthetized prior to surgery by inhalation of 4–5% isoflurane and tails were immersed for 5 min in 37°C saline to dilate the blood vessels. The distal 3 mm of the tail was removed with a scalpel and the tail was immersed in 37°C saline. Times reported represent the time from immersion in saline to the point when primary blood flow was no longer seen; these experiments were stopped after 10 min to minimize blood loss and trauma to the mice. The volume of blood loss was measured by comparing the absorbance at 560 nm of 1 ml of buffer obtained after 10 min of bleeding from the tail with a standard curve constructed from absorbencies of known volumes of blood (Jirouskova *et al*, 2007).

Platelet enumeration and flow cytometric measurement of reticulated platelets

Peripheral blood was collected from the retro-orbital sinus cavity of mice and platelets were enumerated using a Unopette capillary blood collection system (Becton Dickinson, Franklin Lakes, NJ, USA) as described (Konieczna *et al*, 2008; Wang *et al*, 2009). Cytometric detection [using a FACSAria flow cytometer (BD Biosciences, San Jose, CA) with FACSDiva software (BD Biosciences)] of reticulated platelets used thiazole orange, as described (Ault *et al*, 1992). Briefly, whole blood was stained with thiazole orange and anti-CD41 phycoerythrin (PE). Forward scatter, photomultiplier tube/sideways scatter and CD41 expression was used to establish platelet gates and the percentage of thiazole orange incorporation was assessed.

Design of microRNA-adapted shRNAs. RNAi-mediated AHR knockdown experiments used lentiviral vectors for the delivery of microRNA-adapted shRNAs (shRNA-mir) that were designed and produced using the reagents and protocols included in the BLOCK-iT Lentiviral Pol II miR RNAi Expression System (Invitrogen, Carlsbad, CA, USA) as previously described (Fuhrken *et al*, 2008a). To control against off-target silencing effects, independent pre-miRNA inserts were designed to compliment regions at least 200 bases apart in the AHR mRNA. A scrambled control pre-miRNA designed not to target any known human gene (NegA) was used as a negative control. Pre-miRNA sequences used for construction of lentiviral microRNA vectors are as follows:

AHR-A: 5'-TGCTGATATGAAGCACCTCTCCATTAGTTTTGGCCACTGACTGACTAATGGAGGTGCTTCATAT-3'; AHR-B 5'-TGCTGTCATGTTTCAGGATAGTATCAGTTTTGGCCACTGACTGACTGATACTACTGAAACATGA3'; NegA 5'-TGCTGAAATGTAAGTACTGCGCGTGGAGACGTTTTGTGACTGACTGCTCCACGCAGTACATTT-3'; HES1-A: 5'-TGCTGTTTGA TGACTTTCTGTGCTCAGTTTTGGCCACTGACTGACTGAGCACAAAGTCATCAAA-3'; and HES1-B: 5'-TGCTGTTCACTGTCATTTCCAGAAATGGTTTTGGCCACTGACTGACCATTCTGGATGACAGTGAA-3'. The mature microRNA sequence (reverse complement of the target sequence in the target mRNA) is underlined.

Lentiviral production and transduction of CHRF cells

After sequence verification, pLenti6/EmGFP-pre-microRNA viral constructs were used to transduce CHRF cells as described (Fuhrken *et al*, 2008a). After overnight incubation, cells were diluted with growth media and maintained between 50 000 and 1×10^6 cells/ml. At 3–5 d post-transduction, EmGFP⁺ cells were purified by flow cytometric cell sorting.

Flow cytometric analysis of Mk ploidy

All flow cytometry data were acquired using the FACSaria flow cytometer. Ploidy assays were performed using previously published methods with minor modifications (Herault *et al*, 1999; Yang *et al*, 2002). For ploidy analysis of CHRF and murine Mk cultures, cells were fixed for 15 min at room temperature in 0.5% paraformaldehyde in PBS and permeabilized for 1 h at 4°C in 70% methanol. RNA was digested by 15 min of RNase treatment at 37°C and DNA was stained with 50 µg/ml propidium iodide (PI) in PBS at room temperature. In CHRF experiments, we limited our focus to EmGFP⁺ events. Polyloid murine Mks were defined as events with high forward scatter, positive CD41 expression and $\geq 8N$ DNA content.

Flow cytometric analysis of DNA synthesis and Mk apoptosis

DNA synthesis was assessed using a flow cytometric BrdU incorporation assay (Fuhrken *et al*, 2008a). To simultaneously assess DNA synthesis, ploidy and apoptosis, cells were intracellularly labelled with allophycocyanin (APC)-conjugated anti-BrdU and PE-conjugated-anti-cleaved caspase-3 antibodies, treated with RNase and counterstained with 7-Aminoactinomycin D (7-AAD) in parallel experiments, as described (Fuhrken *et al*, 2008a).

Statistical analysis. Tests for statistical significance were performed using Student's *t*-test for independent samples applied to individual time points. For these studies, *P* values ≥ 0.05 were deemed of statistical significance.

Results

AHR-null mice exhibit defects in platelet number and function

To determine if *AHR* expression has an impact on *in vivo* megakaryopoiesis and platelet function, we investigated the steady-state haematological properties of *AHR*-null mice (Schmidt *et al*, 1996). These mice have been used extensively in toxicological studies investigating the mechanisms of action of several exogenous *AHR* ligands, and have shown a role for *AHR* during liver development (Bunger *et al*, 2003). Although *AHR* appears to influence immune function and T-cell regulation (Stevens *et al*, 2009), few published studies have examined other haematological defects of *AHR*-null mice. In the current study, *AHR*-null mice exhibited a 9% decrease and *AHR*^{+/-} mice exhibited a 6% decrease in platelet counts compared to WT mice (Fig 1A). There were also 10.4% fewer reticulated young, RNA-containing platelets in *AHR*-null or *AHR*^{+/-} mice compared to WT mice, indicating a defect in either platelet generation or Mk maturation (Fig 1B). We examined platelet functionality and found that while the average bleeding time for WT mice was approximately 1.5 min, *AHR*-null mice bled for an average of 8 min, or roughly 5.3 times longer (Fig 1C). We also calculated the volume of blood loss and found that *AHR*-null mice lost three times as much blood during these assays as WT mice; *AHR*^{+/-} mice lost twice as much (Fig 1D). To investigate if these platelet defects were due to abnormal Mk maturation, we examined the level of steady-state polyploidization of Mks residing within the murine bone marrow niche. Although decreased *AHR* expression did not impact the frequency of steady-state CD41-expressing cells (data not shown), we found that compared to WT mice, *AHR*^{+/-} and *AHR*-null mice had approximately 25% fewer high ploidy ($\geq 32n$) Mks, but more Mks in the lower ploidy classes of 8n and 16n (Fig 1E). Together, these data suggest that *AHR*-null mice exhibit platelet defects of both number and function, and steady-state Mks from *AHR*-null mice are less polyploid than WT mice.

AHR mRNA expression increases during ex vivo megakaryocytic differentiation, but not during isogenic granulocytic or erythroid differentiation

To verify that increased *AHR* expression was unique to megakaryocytic differentiation, primary human CD34⁺ cells from two separate donors were independently *ex vivo* differentiated toward the Mk, granulocytic and erythroid lineages. To increase the purity of Mks in these cultures we only used Tpo to differentiate the cells toward the Mk lineage (the previously published microarray experiments used a cytokine cocktail to increase the expansion of Mk progenitor cells). In parallel experiments, mRNA was harvested at various time points from CD34⁺ cells collected from two separate donors and used in Q-RT-PCR analysis (*n* = 4). These data demon-

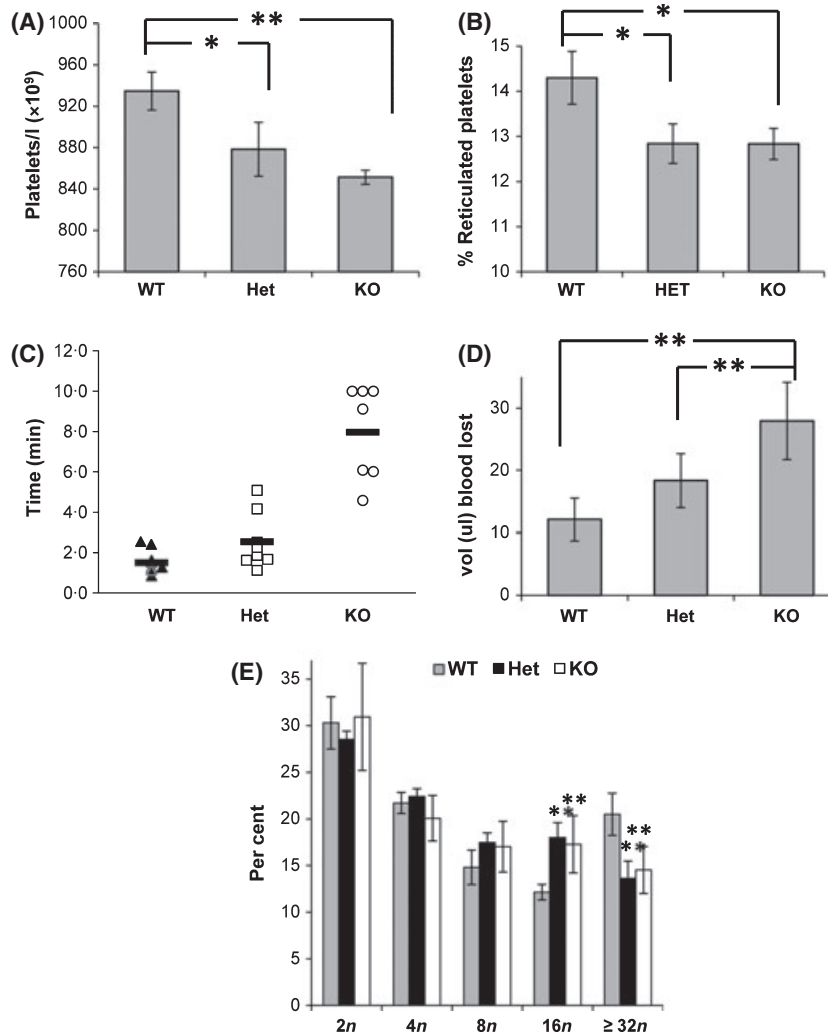


Fig 1. *AHR* null mice exhibit platelet defects and decreased steady-state Mk polyploidization. Peripheral blood from wild type (WT), *AHR*^{+/-} (Het) and *AHR*-null (KO) mice was collected and examined for (A) platelet counts and (B) percentage of reticulated platelets. WT (black triangles), *AHR*^{+/-} (open squares) and *AHR*-null mice (open circles) were subjected to bleeding time assays ($n = 8$ for WT and *AHR*^{+/-}; $n = 7$ for *AHR*-null); shown is (C) the duration of the primary bleed and (D) average volume of blood lost during these experiments. A horizontal line indicates the average bleeding time for each genotype. (E) Bone marrow mononuclear cells were isolated and DNA content of CD41⁺ cells from WT, *AHR*^{+/-} and *AHR*-null mice was examined by flow cytometry. Error bars for all experiments in this figure represent the SEM ($n = 8$). Asterisks denote statistically significant differences compared to WT mice; a single asterisk (*) represents $P < 0.05$ and two asterisks (**) represent $P < 0.01$.

stated that *AHR* mRNA expression increased 3.6-fold during *ex vivo* Mk differentiation from primary human CD34⁺ cells when normalized to the housekeeping genes *GUSB* and *RPLP0* (Fig 2A). *AHR* granulocytic expression decreased by 1.7-fold on day 12 and steadily declined as granulocytic differentiation progressed (10-fold less by day 19, data not shown). By day 12, Mks expressed 6.2-fold more *AHR* mRNA than parallel granulocytic cultures (Fig 2C). *AHR* expression remained statistically unchanged in erythrocytic cultures. The expression pattern of *HES1*, an *AHR* target gene (Thomsen *et al*, 2004), was very similar to *AHR* for all cell lineages studied, although increased *HES1* expression appeared to lag behind *AHR* (Fig 2B). *HES1* expression increased 2.5-fold during Mk differentiation, decreased 2.5-fold during granulopoiesis and remained statistically unchanged during erythrocyte differen-

tiation. By day 12, Mks were expressing 6.2-fold more *HES1* than isogenic granulocytes (Fig 2D). These data indicate that expression of *AHR* and its target gene *HES1* is preferentially upregulated in response to Tpo-induced Mk differentiation, and that *AHR* upregulation is not a general consequence of haematopoietic differentiation, but rather part of the transcriptional machinery specifically responsible for Mk differentiation and maturation.

Treatment of murine myeloid progenitor cells with the prototypical AHR ligand TCDD results in increased megakaryocytic polyploidization

To investigate the possibility that *AHR* could impact Mk differentiation and maturation, we isolated myeloid progenitor

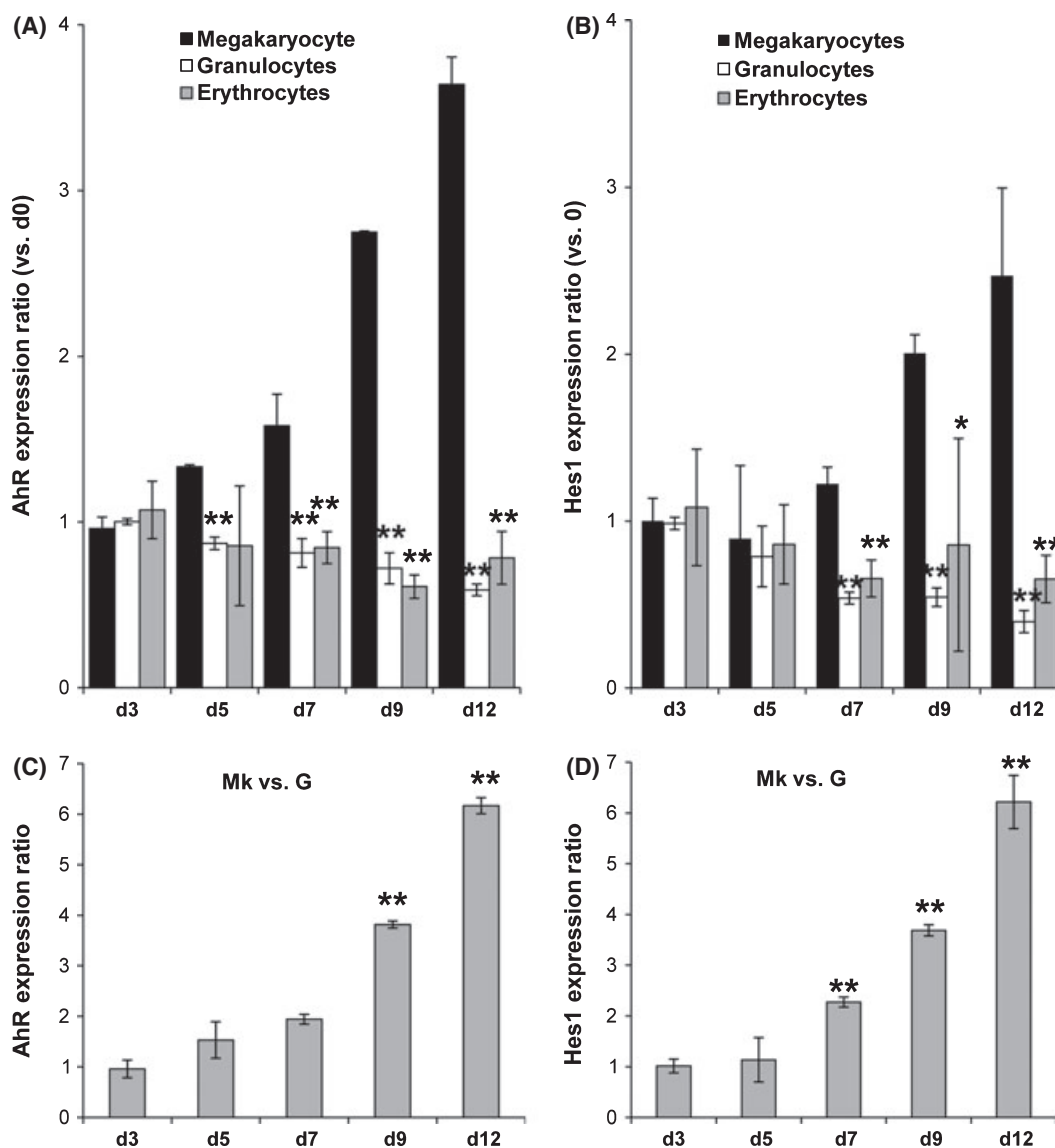


Fig 2. *AHR* mRNA increases during *ex vivo* megakaryopoiesis of primary human CD34⁺ cells undergoing Tpo-stimulated megakaryopoiesis. Q-RT-PCR analysis ($n = 4$) of (A) *AHR* and (B) *HES1* mRNA expression in differentiating primary megakaryocytes, granulocytes and erythrocytes deriving from human CD34⁺ cells from two separate donors. Values were normalized to the housekeeping genes *GUSB* and *RPLP0*. Comparative analysis of (C) *AHR* and (D) *HES1* mRNA expression in megakaryocytes (Mk) relative to isogenic granulocytic (G) cultures from the same day. Error bars represent the SEM for all experiments in this figure. Asterisks denote statistically significant differences (by students *t*-test) as compared to Mk cultures; a single asterisk (*) represents $P < 0.05$ two asterisks (**) represent $P < 0.01$.

cells from the bone marrow of WT mice and investigated the degree of megakaryocytic polyploidization resulting from treatment with the prototypical AHR ligand 2,3,7,8-Tetrachlorodibenzodioxin (TCDD). These myeloid progenitor cells were *ex vivo* expanded in the presence of either 10 nmol/l TCDD, DMSO (vehicle control), or Tpo and the DNA content of the cells was determined by flow cytometry. Although treatment with DMSO alone did result in polyploidization, the cells grew very poorly in culture and very few cells survived to day 10 (data not shown). Importantly, in addition to increased survivability, TCDD treatment resulted in a marked increase in very highly polyploid cells ($\geq 16n$) compared to vehicle

controls, but was not as potent at inducing Mk polyploidization as 100 ng/ml Tpo (Fig 3A).

AHR protein expression levels increase and *AHR* translocates from the cytoplasm to the nucleus during megakaryocytic differentiation

Differential RNA and protein stability frequently result in mRNA expression levels that do not accurately portray the protein abundance of a given gene product within cells. Therefore, the protein-level expression of AHR in PMA-differentiated CHRF cells was examined. Initial experiments

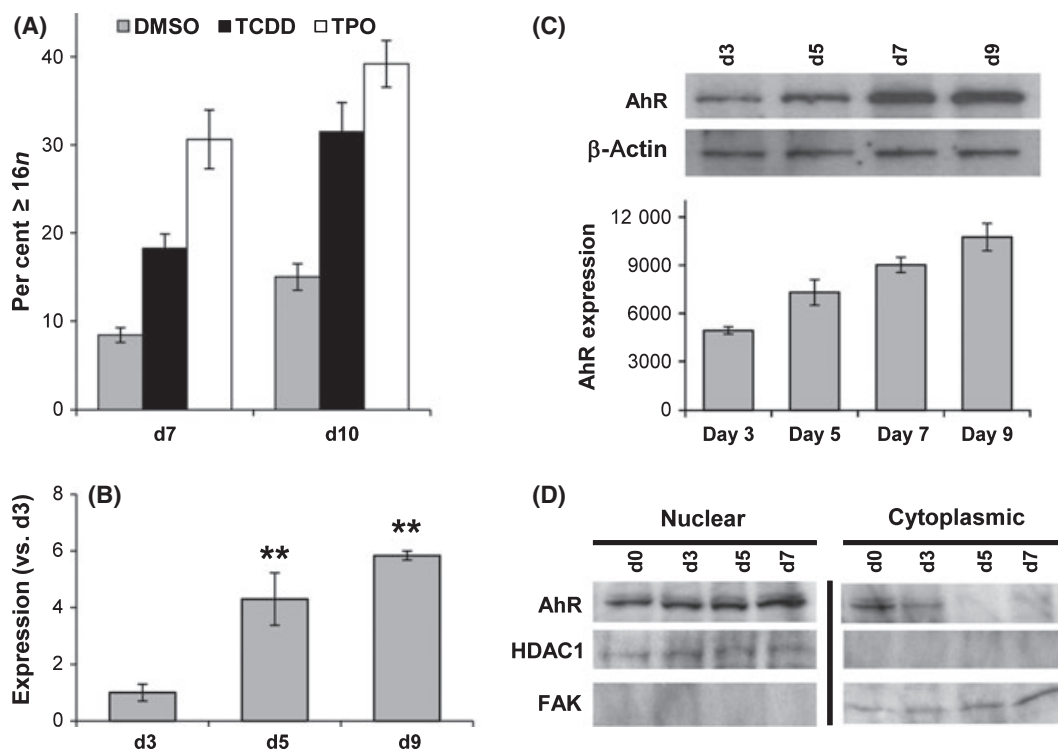


Fig 3. TCDD induces polyploidization of *ex vivo* cultured primary murine Mks; AHR protein levels increase during *ex vivo* megakaryopoiesis and is predominantly localized in the nucleus in differentiated Mks. (A) Murine bone marrow progenitors were *ex vivo* expanded in the presence of either dimethyl sulfoxide (DMSO), 10 nmol/l tetrachlorodibenzodioxin (TCDD), or thrombopoietin (TPO) and DNA content was assessed by flow cytometry; shown is the percentage of very high ploidy ($\geq 16n$) cells. (B) Q-RT-PCR analysis ($n = 3$) of *AHR* mRNA expression in differentiating CHRF cells. Values were normalized to housekeeping genes *GUSB* and *RPLP0* mRNA expression. (C) Western blot analysis ($n = 3$) of AHR protein expression during CHRF megakaryopoiesis. Densitometry values were normalized to housekeeping protein expression (beta-actin) (D) In separate experiments ($n = 3$), nuclear and cytoplasmic fractions were obtained from differentiating CHRF cells and used in Western blot analysis. Error bars represent the SEM for all experiments in this figure. Asterisks denote statistically significant differences as compared to undifferentiated CHRF cultures; a single asterisk (*) represents $P < 0.05$ two asterisks (**) represent $P < 0.01$.

verified that PMA-induced megakaryopoiesis of CHRF cells produced a similar upregulation of AHR expression, resulting in a 5.8-fold increase in *AHR* mRNA (Fig 3B). Western Blot analysis of whole cell lysates ($n = 3$) indicate that increased *AHR* mRNA levels were accompanied by a 2.2-fold increase of AHR protein abundance during CHRF Mk differentiation (Fig 3C). Increased protein abundance of a transcription factor does not necessarily result in increased transcriptional activity. Oftentimes, transcription factors are sequestered away from nuclear DNA target genes and relegated to the cytosol when not actively transcribing target genes. To investigate if Mk differentiation coincides with AHR nuclear translocation from the cytoplasm to the nucleus, nuclear and cytoplasmic extracts were generated from CHRF cells undergoing PMA-mediated Mk differentiation. In these experiments ($n = 3$), AHR nuclear expression increased by 67% as megakaryopoiesis progressed, while AHR cytoplasmic expression decreased 10-fold (Fig 3D). This indicates that in addition to being specifically upregulated during Mk differentiation, AHR translocates from the cytoplasm to the nucleus as Mks differentiate.

AHR DNA binding increases during CHRF Mk differentiation

Because AHR translocated to the nucleus during Mk differentiation and AHR-null mice exhibited platelet defects, we next investigated AHR transcriptional activity during megakaryocytic differentiation. Specifically, we measured the binding of nuclear lysate proteins from differentiating CHRF cells to an AHR consensus binding sequence in Electromobility shift assays (EMSA). Nuclear extracts from Mk-differentiated CHRF cells were isolated and incubated with biotinylated AHR-consensus binding sequence oligonucleotides (Panomics). Band specificity was ascertained during competition assays in which nuclear extracts were pre-incubated with unlabeled oligonucleotides. We used the consensus AHR binding sequence to capture general, unbiased binding patterns; binding to a specific AHR target gene promoter was assessed later. As shown in a representative experiment, we identified a low mobility DNA/protein complex that increased 2.4-fold during CHRF differentiation and was disrupted during competitor assays (Fig 4A). This experiment suggested

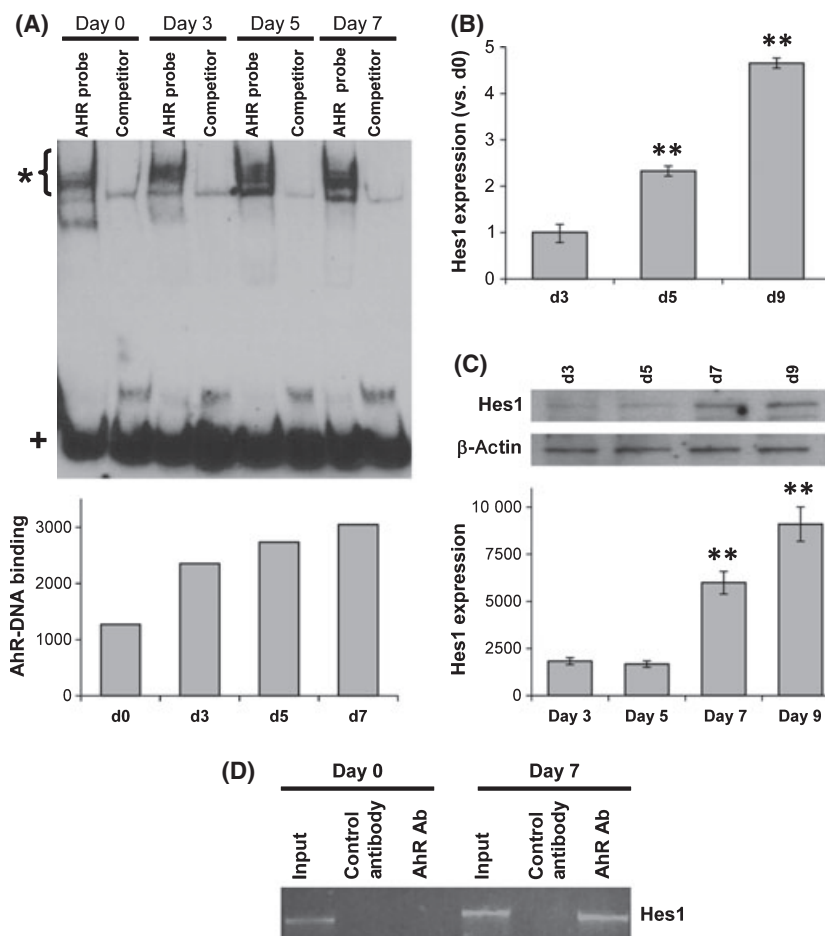


Fig 4. AHR DNA binding and HES1 expression increases during CHRF megakaryocytic differentiation. (A) A representative EMSA experiment ($n = 4$) used nuclear extracts from differentiating CHRF cells and was incubated with biotinylated AHR consensus binding sequence oligonucleotides. During competition assays, nuclear extracts were pre-incubated with unlabeled AHR consensus binding sequence oligonucleotides to ascertain band specificity. The region marked with an asterisk (*) was used in subsequent densitometry analysis using imageJ software and free probe is indicated by a plus sign (+). (B) Q-RT-PCR experiments ($n = 3$) examined *HES1* mRNA expression (a known AHR transcriptional target) after PMA-induced Mk differentiation of CHRF cells. Values were normalized to housekeeping gene expression (*GUSB* and *RPLP0*) to minimize loading differences and compared to undifferentiated (d0) cells. (C) Western blots using total cell lysates from differentiating CHRF cells examined protein expression of HES1 ($n = 3$); a representative Western blot of PMA differentiated CHRF whole cell lysates is shown. Densitometry values were normalized to housekeeping gene expression using ImageJ software. Error bars represent the SEM. Asterisks denote statistically significant differences as compared to undifferentiated CHRF cultures; a single asterisk (*) represents $P < 0.05$ two asterisks (**) represent $P < 0.01$. (D) CHRF cells were analyzed by chromatin immunoprecipitation (IP) for *in vivo* AHR binding to the *HES1* promoter. Total input (non-precipitated) chromatin was used as a positive control, and chromatin coprecipitating with antibodies toward Immunoglobulin G was used as a negative control in these experiments.

that AHR may bind the DNA and regulate the expression of target genes during megakaryopoiesis.

Gene expression of the AHR target HES1 increases during megakaryocytic differentiation

Our previous EMSA experiments used an AHR consensus binding sequence, so we chose to investigate gene expression of *HES1*, a known AHR transcriptional target (Thomsen *et al*, 2004). In addition to being upregulated during megakaryopoiesis (Fig 2B), *HES1* may be relevant to Mk differentiation because it is known to regulate Notch signaling and cell cycle

progression (Murata *et al*, 2005), both of which are intimately involved in megakaryocytic differentiation. In agreement with our data using CD34-derived primary Mks, *HES1* mRNA expression increased 4.7-fold by day 9 of CHRF Mk differentiation compared to undifferentiated cells (Fig 4B; $P \leq 0.01$). *HES1* protein expression increased 4.6-fold by day 9 of CHRF Mk differentiation (Fig 4C; $P \leq 0.01$). Chromatin immunoprecipitation confirmed that AHR directly activated *HES1*, but only in CHRF cells differentiating toward the Mk lineage (Fig 4D). These data, coupled with our EMSA results, support the hypothesis that increased AHR DNA binding impacts AHR target gene expression during megakaryopoiesis.

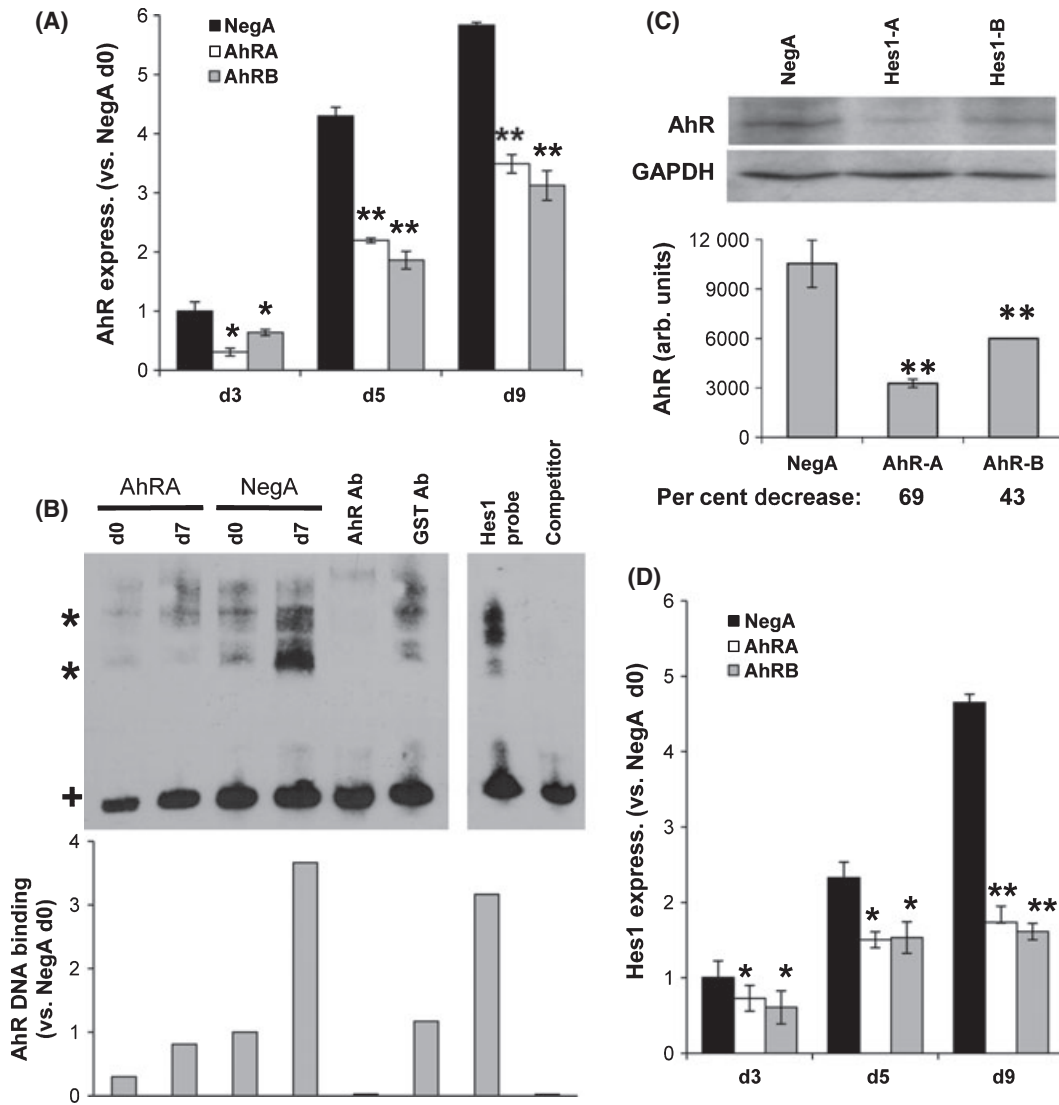


Fig 5. AHR knockdown effectively decreases AHR expression and activity in CHRF cells. (A) Q-RT-PCR experiments ($n = 3$) investigated AHR expression in NegA, AHR-A and AHR-B cell lines and were normalized to housekeeping genes. (B) A representative Western Blot of AHR protein expression in stable AHR-A and AHR-B CHRF cell lines, as compared to scrambled control ($n = 3$). Densitometry values used in this figure were normalized to GAPDH expression using ImageJ software. (C) Nuclear extracts from either undifferentiated or PMA-differentiated knockdown CHRF cell lines were used in EMSA experiments ($n = 3$) and were incubated with biotinylated oligonucleotides corresponding to the putative AHR binding sequence within the *HES1* promoter. Sequence specificity was determined during competition assays using unlabeled oligonucleotides; protein specificity was determined by pre-incubation with antibodies to AHR. The regions marked with an asterisk (*) were used in subsequent densitometry analysis and normalized to free probe, indicated by a plus sign (+). (D) *HES1* mRNA expression was determined by Q-RT-PCR analyses ($n = 3$) in NegA, AHR-A and AHR-B cell lines. Densitometry values were normalized to housekeeping gene expression using ImageJ software. Error bars represent the SEM. Asterisks denote statistically significant differences compared to NegA cells from the same day of PMA-induced differentiation; a single asterisk (*) represents $P < 0.05$ and two asterisks (**) represent $P < 0.01$.

Generation of AHR knockdown (KD-AHR) CHRF cell lines

To investigate the impact of AHR expression on Mk differentiation, GFP-tagged replication-incompetent lentiviruses were used to stably express shRNA-mir in CHRF cells to knockdown AHR expression. Transduced RNAi-mediated KD-AHR CHRF cells were subsequently sorted for GFP⁺ cells via flow cytometry (enriched >98%, data not shown) and

expanded, resulting in stable CHRF cell lines expressing between 37% and 69% less AHR than cells expressing a scrambled control sequence (NegA) after 3 d of PMA-induced Mk differentiation (Fig 5A). Although Mk differentiation resulted in increased AHR expression in the KD-AHR CHRF cells, by day 9 they expressed between 40% and 46% less AHR mRNA than CHRF cells expressing the scrambled control sequence (Fig 5A). Western blot analyses confirmed significant AHR protein reduction in both KD-AHR CHRF cell lines.

AHR-A resulted in a 69% decrease in AHR protein expression, while AHR-B resulted in a 43% decrease (Fig 5B).

KD-AHR CHRF cells exhibit impaired AHR transcriptional activity

EMSA experiments using a biotinylated sequence flanking the putative AHR binding site within the *HES1* promoter identified two low mobility complexes that formed upon incubation with nuclear proteins. The vast majority of binding to this region of the *HES1* promoter was ablated by antibodies directed toward AHR, indicating that AHR is present within the low mobility complex; the specificity of the low mobility DNA/protein complex that formed upon incubation with the *HES1* probe was determined in separate competition assays (Fig 5C). Undifferentiated KD-AHR cells had 70% less complex formation than control cells, indicating that the ability of AHR to function as a transcription factor was significantly impacted in the KD-AHR cells used in our experiments. Binding to the AHR consensus sequence increased after Mk differentiation in both KD-AHR and control CHRF cells, but on day 7 KD-AHR CHRF cells exhibited 3-7-fold less binding compared to NegA cells (Fig 5C). Decreased AHR DNA binding in KD-AHR CHRF cells resulted in an impaired mRNA expression of the AHR target gene *HES1*. After 3 d of PMA-induced Mk differentiation KD-AHR CHRF cells expressed between 27% and 40% less *HES1* mRNA than NegA control cells for AHR-A and AHR-B respectively (Fig 5D). By day 9 the difference was more dramatic; AHR-A cells and AHR-B cells expressed 63% and 68% less *HES1* mRNA, respectively.

KD-AHR CHRF cells exhibit decreased polyploidization during megakaryopoiesis

To examine if reduced AHR expression impacts Mk polyploidization, KD-AHR CHRF cells were differentiated toward the Mk lineage with PMA and the degree of polyploidization was measured by flow cytometry as the cells differentiated over 9 d of culture. Based on its involvement in cell cycle regulation, we hypothesized that decreased AHR expression would decrease CHRF polyploidization as Mk differentiation progressed. In these experiments ($n = 3$ for each construct), the fraction of AHR-A and AHR-B CHRF cells that were polyploid ($\geq 8n$) was significantly decreased at every time point examined upon PMA differentiation compared to NegA expressing cells (Fig 6A; $P < 0.05$ for every time point).

As shown in a representative experiment, 36% of the NegA CHRF cells were polyploid 7 d after PMA-induced Mk differentiation (the highest point), while AHR knockdown resulted in less than 14% of the cells becoming polyploid by day 7 (2.7-fold difference; Fig 6B). Supporting the hypothesis that AHR is involved in Mk polyploidization, the ploidy distributions in KD-AHR CHRF cells were clearly shifted toward lower ploidy and KD-AHR CHRF cells were incapable of reaching higher ploidy classes (i.e. $>16n$) observed in

control cells (Fig 6B). Similar results were obtained using the AHR-A construct (data not shown). There were no differences in ploidy distribution between undifferentiated control or KD-AHR CHRF cells and all cell lines were 0-4% polyploid (Fig 6C; $n = 6$) indicating that knocking down AHR does not result in aberrantly decreased ploidy levels. Decreased AHR expression also did not result in statistically significant changes in proliferation (measured by cell counts, data not shown) or DNA synthesis in undifferentiated CHRF cells as measured by BrdU incorporation (Fig 6D). BrdU incorporation, as indicated by adding P₁ and P₂, was 40-0% and 42-9% for AHR-A and AHR-B respectively as compared to 43-3% for NegA.

Reduced AHR expression results in increased DNA synthesis, but does not impact Mk apoptosis

We used a flow-cytometric BrdU incorporation assay to investigate DNA synthesis during polyploidization of PMA-differentiated CHRF cells; our experimental design allowed us to investigate DNA synthesis within discrete ploidy classes (i.e. $2n$, $4n$, etc.). Shown are representative BrdU plots from day 5 of PMA-induced Mk differentiation of the various CHRF cell lines. In these experiments, AHR knockdown resulted in a 11% increase in proliferation (based on cell counts; data not shown), and twice as much BrdU incorporation, represented by adding the events in gates P₁ and P₂, as NegA CHRF cells (Fig 7A; approximately 30% compared to 16% for NegA cells). We simultaneously investigated the degree of polyploidization in these cells. As indicated by PI histograms, NegA CHRF cells had twice as many polyploid cells as KD-AHR CHRF cells on day 5 of PMA-induced differentiation (Fig 7B; approximately 16% compared to 8%). BrdU incorporation was higher in KD-AHR CHRF cells after PMA-induced differentiation; 5 d after PMA-induced Mk differentiation KD-AHR cells had on average twice as many BrdU positive cells as the NegA CHRF cell line (Fig 7C). Interestingly, on average across all time points, AHR knockdown resulted in 2-3-fold fewer polyploid BrdU⁺ cells than the control NegA cell line, indicating that most BrdU incorporation occurred in low ploidy cells (Fig 7D).

Changes in ploidy level can be attributed to either increased DNA synthesis or decreased apoptosis, so we also examined the levels of apoptosis in differentiating knockdown cell lines by assessing the amount of activated caspase-3 (Fuhrken *et al*, 2008a) at various time points during Mk differentiation. The results of these experiments showed no statistically significant differences in the level of active caspase-3 (Fig 7E). Taken together, these data suggest that AHR regulates Mk polyploidization during differentiation, but does not impact apoptosis.

KD-HES1 CHRF cells exhibit decreased polyploidization during megakaryopoiesis

Our data suggested that AHR impacts Mk ploidy through the regulation of its transcriptional target *HES1*. To examine the

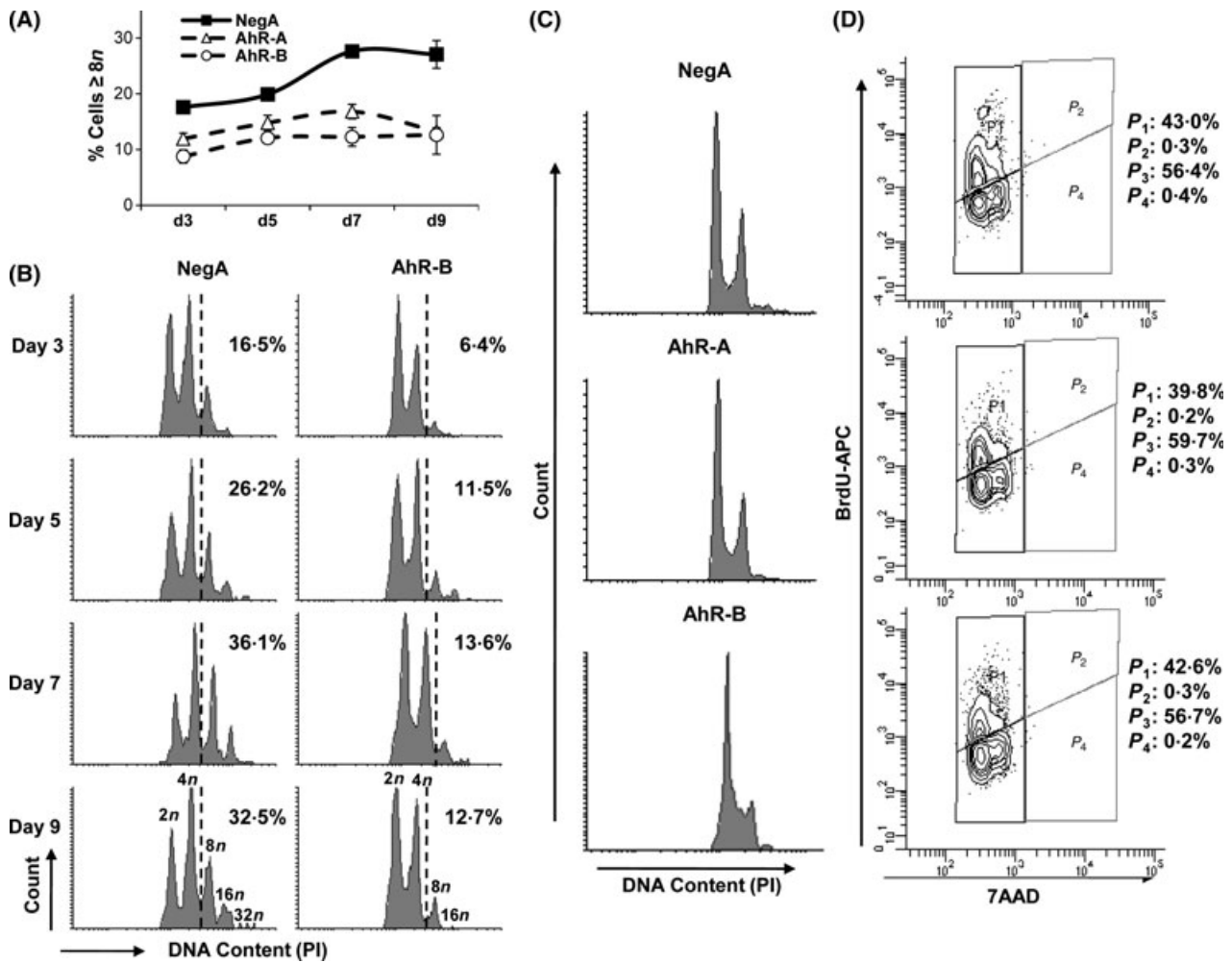


Fig 6. AHR knockdown leads to decreased polyploidization. (A) DNA content was assessed by flow cytometry on the days indicated and the percentage of high-ploidy ($\geq 8N$) cells among all cells was reported for NegA (black squares), AHR-A (open triangles) and AHR-B (open circles) CHRF cells. Error bars represent the SEM ($n = 3$ for each cell line). (B) DNA histograms from a representative experiment at the designated time-points. Dashed lines indicate high ploidy ($\geq 8n$) cells and the percent polyploidization is indicated. (C) DNA content and (D) BrdU incorporation was assessed in undifferentiated NegA, AHR-A and AHR-B CHRF cell lines by flow cytometry.

likelihood of this model, we employed a genetic approach and used RNAi to generate knockdown *HES1* CHRF cell lines (KD-*HES1*). We reasoned that if AHR impacts Mk polyploidization through interactions with *HES1*, then RNAi-mediated *HES1* knockdown should reduce Mk ploidy, similar to that seen in KD-AHR cells.

We first employed Q-RT-PCR to verify the efficiency of our RNAi-mediated gene knockdown. The KD-*HES1* cell lines generated expressed 68% and 59% less *HES1* mRNA (Fig 8A; $n = 3$; $P = 0.008$ for *HES1*-A and $P = 0.015$ for *HES1*-B). Importantly, knocking down *HES1* did not impact expression of *AHR* (data not shown; $n = 3$, $P = 0.46$ for both KD-*HES1* cell lines). Analysis of Western blots ($n = 3$) showed that these changes in *HES1* mRNA resulted in 31% and 47% less *HES1* protein expression for *HES1*-A and *HES1*-B respectively (Fig 8B). Although there was no impact on proliferation or the degree of polyploidization in undifferentiated cells (data not shown), KD-*HES1* CHRF cells were significantly less

polyploid throughout megakaryopoiesis; by day 7 of PMA-induced Mk differentiation both KD-*HES1* cell lines were 31% less polyploid than control CHRF cells (Fig 8C, $P < 0.05$ for all time points). Similar to knocking down AHR, KD-*HES1* cells were 15% more proliferative (data not shown), had Mk-ploidy distributions that were shifted towards lower ploidy classes and were incapable of reaching higher ploidy classes (i.e. $\geq 32n$) seen in control cells. Although there was little impact in undifferentiated CHRF cells, ploidy levels on day 7 (maximal ploidy in control cells) were between 25.3% and 26.7% less than control cells depending on the cell line ($n = 3$; $P < 0.05$ for both cell lines).

Discussion

Because AHR may be activated during cellular differentiation of many lineages, we investigated the lineage specificity of haematopoietic AHR activation. Several haematopoietic

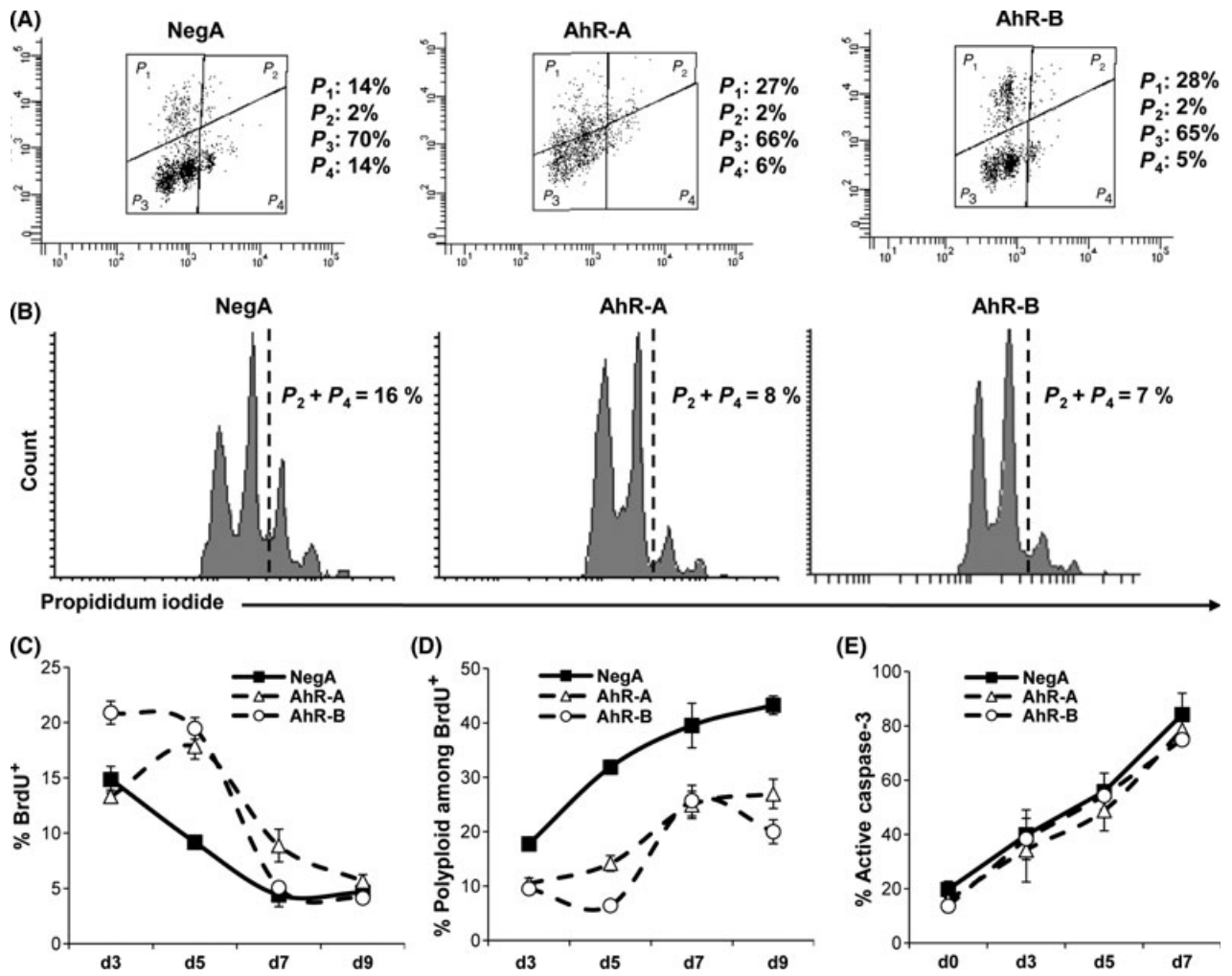


Fig 7. AHR knockdown results in increased DNA synthesis of low ploidy cells without influencing apoptosis of differentiating CHRF cells. BrdU incorporation was used to investigate the role of AHR down regulation on the cell cycle of PMA-differentiated NegA, AHR-A and AHR-B cells ($n = 3$ for each cell line). (A) Representative experiments after 5 d of PMA-induced differentiation and their (B) corresponding ploidy histograms. Dashed lines indicate high ploidy ($\geq 8n$) cells; percent polyploidization ($P_2 + P_4$) is indicated. (C) BrdU incorporation ($P_1 + P_2$) was analyzed during PMA-induced differentiation of NegA (black squares), AHR-A (open triangles) and AHR-B (open circles) cells. (D) A further analysis of the data investigated the percentage of BrdU⁺ cells that were polyploid [$P_2/(P_1 + P_2)$]. (E) Caspase-3 activity was assessed as a measure of apoptosis in differentiating CHRF cell lines. Error bars represent the SEM.

lineages are impacted by exposure to toxicological ligands (notably monocytes, T-cells and B lymphocytes), but here, there is no exposure to such ligands. We performed parallel cultures of isogenic primary human CD34⁺ cells undergoing megakaryocytic, granulocytic and erythroid differentiation (Fig 2A–D) and found that *AHR* mRNA expression increased during *ex vivo* Mk differentiation, but not during isogenic granulocytic or erythrocytic differentiation (Fig 2). *AHR* mRNA expression increased 3–6-fold during *ex vivo* Mk differentiation, but steadily declined during *ex vivo* granulocytic differentiation. By day 12, *AHR* expression had decreased by 1–7-fold and steadily declined as granulocytic differentiation progressed (10-fold less by day 19). *AHR* expression remained statistically unchanged in parallel erythrocytic cultures. These data indicate that *AHR* upregulation is not a general conse-

quence of haematopoietic differentiation, but rather part of the transcriptional machinery responsible for Mk differentiation and maturation. In addition, we show *in vivo* and *in vitro* data that demonstrate a functional impact upon Mk differentiation and maturation when AHR expression is reduced. As such, it is difficult to argue that the phenomenon we describe is either non-specific or trivial.

Although we observed only modest (but statistically significant) differences in platelet counts between WT, *AHR*-null and *AHR*^{+/-} mice, our findings are similar to those found with the CDK inhibitor CDKN1A (p21/WAF1). For example, it is now widely recognized that CDKN1A has a crucial role during megakaryocytic differentiation, yet *Cdkn1a*^{-/-} mice have relatively normal steady-state platelet levels and impact Mk mainly by influencing the degree of Mk polyploidization

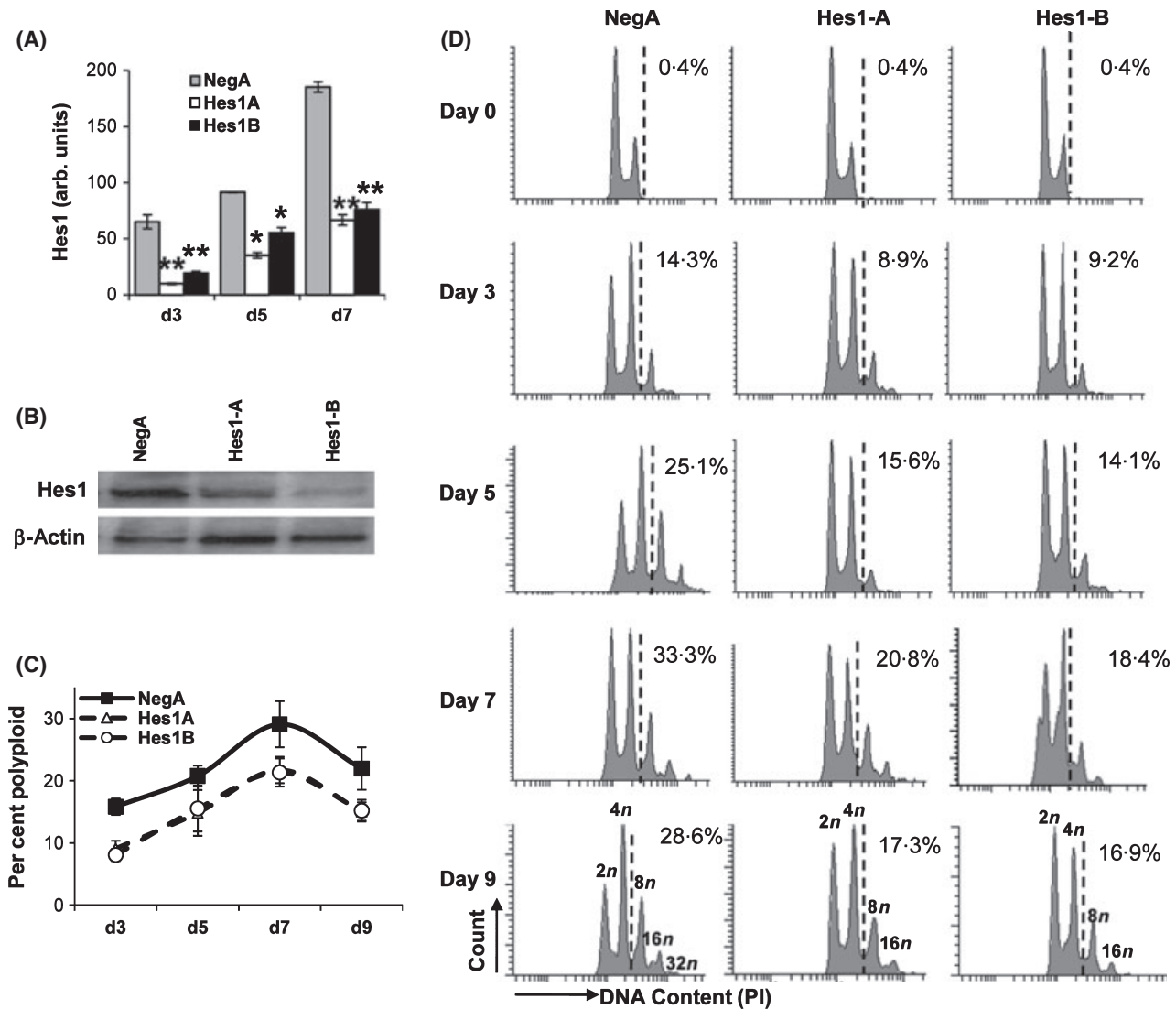


Fig 8. HES1 knockdown leads to decreased polyploidization. (A) Q-RT-PCR experiments ($n = 3$) investigated *HES1* mRNA expression in NegA, HES1-A and HES1-B cell lines and were normalized to housekeeping genes (*GUSB* and *RPL0*). (B) A representative Western Blot of HES1 protein expression in stable HES1-A and HES1-B CHRF cell lines, as compared to scrambled control ($n = 3$). (C) DNA content was assessed by flow cytometry on the days indicated and the percentage of high-ploidy ($\geq 8N$) cells was reported for NegA (black squares), HES1-A (open triangles) and HES1-B (open circles) cells. Error bars represent the SEM ($n = 4$ for each cell line). (D) DNA histograms from a representative experiment at the designated time-points after PMA-induced Mk differentiation. Dashed lines indicate high ploidy ($\geq 8n$) cells and the percentage of polyploidization is indicated. Error bars represent the SEM. Asterisks denote statistically significant differences compared to NegA cells from the same day of PMA-induced differentiation; a single asterisk (*) represents $P < 0.05$ and two asterisks (**) represent $P < 0.01$.

(Baccini *et al*, 2001), similar to the phenotype we see in *AHR*-null mice. Importantly, we found that *AHR*-null mice had 10.4% fewer newly synthesized (reticulated) platelets, a 5.3-fold increase in bleeding times and lost twice as much blood during bleeding time experiments as WT control mice. Interestingly, these results are more dramatic than those seen in *Cdkn1a*-null mice and were in agreement with previous studies of *Oryzias latipes* embryogenesis that suggest *AHR* is critical for blood clotting (Kawamura & Yamashita, 2002). The dramatic differences in the percentage of reticulated platelets, bleeding times and blood volume lost between WT and *AHR*-null mice

are most likely not solely due to abnormal Mk maturation (evidenced by fewer $\geq 32n$ Mks), because the ploidy distribution was essentially identical for *AHR*-null and *AHR*^{+/-} mice, despite the fact that *AHR*^{+/-} mice experienced intermediate *in vivo* platelet defects (Fig 1). Loss of a single copy of the *AHR* gene during our investigations led to many of the *in vivo* platelet defects we observed, namely platelet counts, percentage of reticulated platelets, bleeding times and total blood volume lost. The notion that *AHR* haploinsufficiency leads to megakaryocytic defects is further supported by the data generated from our KD-*AHR* CHRF cell lines, expressing 40–70% less

AHR than control cells. As such, AHR inhibition may provide interesting therapeutic targets for diseases such as thrombocythaemia.

In addition to influencing Mk polyploidization, AHR-deficiency may impact platelet activation, aggregation, or some other aspect of platelet function such as clot formation, thromboxane A2 synthesis, granule secretion. Any of these platelet functions could be impacted by AHR signaling, and as such is beyond the scope of our current investigation, which was designed to interrogate our hypothesis that AHR is a novel regulator of megakaryopoietic polyploidization. We are, however, planning future experiments into the nature of the platelet defects found in AHR-null mice to better understand the role of AHR in platelet function, especially in light of data suggesting that AHR regulates *vav3*, a critical mediator of platelet activation (Fernandez-Salguero, 2010). It is also not clear if the decreased megakaryocytic polyploidization observed in AHR^{-/-} and AHR^{+/-} mice is cell autonomous. Future studies in which bone marrow from AHR^{-/-} donor mice is transplanted into wild type recipient mice could begin to address this issue and delineate AHR effects originating from Mks from signals originating from adjacent endothelial cells.

Knockdown of either AHR or HES1 resulted in significantly less Mk polyploidization throughout differentiation and although not fully investigated in our current study, we feel that AHR could mediate Mk polyploidization through interactions with HES1. HES1 is a known cell cycle regulator and mediator of Notch signaling and our findings are consistent with studies reporting that Notch signaling regulates the initial entry into endomitosis in *Drosophila* by altering cell cycle regulation (Deng *et al*, 2001; Schaeffer *et al*, 2004; Jordan *et al*, 2006) and it is possible that Notch signaling could similarly impact Mk polyploidization. Tpo impacts several of the same signaling pathways as Notch, including ERK/JNK/p38, Rb and E2F (Matsumura *et al*, 1997; Quentmeier *et al*, 1998; Miyazaki *et al*, 2001), supporting a notion of crosstalk between these signaling pathways. Other studies have shown that co-culturing bone marrow-derived Lin⁻Sca-1⁺cKit⁺ haematopoietic stem cells with OP9 cells expressing the Notch ligand Delta-like1 results in large cells that upregulate HES1, undergo polyploidization, and express Mk surface markers (Mercher *et al*, 2008). During these studies, HES1 was more highly expressed in erythroid-Mk progenitor cells than common myeloid or granulocyte-macrophage progenitor cells, suggesting that HES1 has a specific Mk function. Supporting our findings that HES1 expression increases as a result of physiological (Tpo-induced) megakaryocytic differentiation, HES1 expression increased in response to Tpo treatment during *in vivo* investigations of acute megakaryoblastic leukaemia (Mercher *et al*, 2009), and the level of *DLK1* mRNA, a HES1 transcriptional target, is increased in CD34⁺ cells isolated from MDS patients compared to CD34⁺ cells from 11 normal individuals (Sakajiri *et al*, 2005).

However, any speculation into the involvement of HES1 must be tempered with caution. It is important to note that the

AHR regulon is quite extensive, and furthermore, AHR signaling is fairly promiscuous and may be interacting with other signaling pathways. AHR is a member of the PAS (PER-ARNT-SIM) gene family and, as such, shares structural similarity and interacts with members of the circadian clock. Among many other effects, clock genes are known to regulate cell cycle progression (reviewed in Borgs *et al*, 2009). Recent findings have also shown that clock genes block the formation of the contractile ring that forms as *Synechococcus elongatus* divides (Dong *et al*, 2010) – a process that is specifically altered during Mk differentiation, but was not examined in our current studies. Therefore, future work will investigate the AHR regulon using genomic analyses of genes that are differentially expressed in AHR-null mice compared to WT to identify additional mechanisms through which AHR could influence Mk polyploidization.

The timing of transcription factor expression and down regulation is critical to differentiation (Chou *et al*, 2009). As such, we find it interesting that studies using lin⁻sca⁺ haematopoietic stem cells implied that HES1 inhibits GATA1 and sustains GATA2 transcriptional activity (Ishiko *et al*, 2005). While GATA1 is critical to the maturation of Mks, GATA2 seems to control the early stages of haematopoiesis (Tsai *et al*, 1994; Tsai & Orkin, 1997). GATA2 is continuously expressed in Mks, but silenced in erythroid cells (Dorfman *et al*, 1992). Taken together, these data suggest that one function of HES1 may be to maintain an undifferentiated, ‘stem cell-like’ state and appears to contradict our findings. However, while GATA1 expression is critical to the initial lineage decision to become Mks (Shivdasani *et al*, 1997), HES1 may serve an essential role to downregulate GATA1 in late Mk cells. The expression pattern of GATA1 agrees with this, as its expression drops sharply in mature Mks (Fuhrken *et al*, 2008b). HES1 may also assist GATA2 expansion of immature Mks (Huang *et al*, 2009) that have already begun Mk differentiation. Future experiments will investigate these intriguing possibilities in detail.

Acknowledgements

This work was supported by Award Number F32HL091620 from the National Heart, Lung and Blood Institute of the National Institutes of Health (S.L.). The content is solely the responsibility of the authors and does not necessarily represent the official views of the National Heart, Lung and Blood Institute or the National Institutes of Health. The AHR-null mice used in this study were kindly provided by Dr. Christopher Bradfield at the University of Wisconsin School of Medicine and Public Health. We would like to thank our colleagues across the country for their insights and technical assistance during the planning stages of our study. Special thanks to Pani Apostolidis for helpful scientific discussions, help in planning flow cytometry experiments and suggestions throughout this research.

References

- Akahoshi, E., Yoshimura, S. & Ishihara-Sugano, M. (2006) Over-expression of AhR (aryl hydrocarbon receptor) induces neural differentiation of Neuro2a cells: neurotoxicology study. *Environmental Health*, **5**, 24.
- Ault, K.A., Rinder, H.M., Mitchell, J., Carmody, M.B., Vary, C.P. & Hillman, R.S. (1992) The significance of platelets with increased RNA content (reticulated platelets). A measure of the rate of thrombopoiesis. *American Journal of Clinical Pathology*, **98**, 637–646.
- Baccini, V., Roy, L., Vitrat, N., Chagraoui, H., Sabri, S., Le Couedic, J.P., Debili, N., Wendling, F. & Vainchenker, W. (2001) Role of p21(Cip1/Waf1) in cell-cycle exit of endomitotic megakaryocytes. *Blood*, **98**, 3274–3282.
- Boitano, A.E., Wang, J., Romeo, R., Bouchez, L.C., Parker, A.E., Sutton, S.E., Walker, J.R., Flaveny, C.A., Perdew, G.H., Denison, M.S., Schultz, P.G. & Cooke, M.P. (2010) Aryl hydrocarbon receptor antagonists promote the expansion of human hematopoietic stem cells. *Science*, **329**, 1345–1348.
- Borgs, L., Beukelaers, P., Vandenbosch, R., Belachew, S., Nguyen, L. & Malgrange, B. (2009) Cell “circadian” cycle: new role for mammalian core clock genes. *Cell Cycle*, **8**, 832–837.
- Bunger, M.K., Moran, S.M., Glover, E., Thomae, T.L., Lahvis, G.P., Lin, B.C. & Bradfield, C.A. (2003) Resistance to 2,3,7,8-tetrachlorodibenzo-p-dioxin toxicity and abnormal liver development in mice carrying a mutation in the nuclear localization sequence of the aryl hydrocarbon receptor. *Journal of Biological Chemistry*, **278**, 17767–17774.
- Chen, C., Fuhrken, P.G., Huang, L.T., Apostolidis, P., Wang, M., Paredes, C.J., Miller, W.M. & Papoutsakis, E.T. (2007) A systems-biology analysis of isogenic megakaryocytic and granulocytic cultures identifies new molecular components of megakaryocytic apoptosis. *BMC Genomics*, **8**, 384.
- Chou, S.T., Khandros, E., Bailey, L.C., Nichols, K.E., Vakoc, C.R., Yao, Y., Huang, Z., Crispino, J.D., Hardison, R.C., Blobel, G.A. & Weiss, M.J. (2009) Graded repression of PU.1/Sfp1 gene transcription by GATA factors regulates hematopoietic cell fate. *Blood*, **114**, 983–994.
- Deng, W.M., Althausen, C. & Ruohola-Baker, H. (2001) Notch-Delta signaling induces a transition from mitotic cell cycle to endocycle in *Drosophila* follicle cells. *Development*, **128**, 4737–4746.
- Denison, M.S., Fisher, J.M. & Whitlock, Jr, J.P. (1988) The DNA recognition site for the dioxin-Ah receptor complex. Nucleotide sequence and functional analysis. *Journal of Biological Chemistry*, **263**, 17221–17224.
- Dignam, J.D., Lebovitz, R.M. & Roeder, R.G. (1983) Accurate transcription initiation by RNA polymerase II in a soluble extract from isolated mammalian nuclei. *Nucleic Acids Research*, **11**, 1475–1489.
- Dong, G., Yang, Q., Wang, Q., Kim, Y.I., Wood, T.L., Osteryoung, K.W., van Oudenaarden, A. & Golden, S.S. (2010) Elevated ATPase activity of KaiC applies a circadian checkpoint on cell division in *Synechococcus elongatus*. *Cell*, **140**, 529–539.
- Dorfman, D.M., Wilson, D.B., Bruns, G.A. & Orkin, S.H. (1992) Human transcription factor GATA-2. Evidence for regulation of preproendothelin-1 gene expression in endothelial cells. *Journal of Biological Chemistry*, **267**, 1279–1285.
- Fernandez-Salguero, P.M. (2010) A remarkable new target gene for the dioxin receptor: the Vav3 proto-oncogene links AhR to adhesion and migration. *Cell Adhesion and Migration*, **4**, 172–175.
- Fuhrken, P.G., Chen, C., Miller, W.M. & Papoutsakis, E.T. (2007) Comparative, genome-scale transcriptional analysis of CHR-288-11 and primary human megakaryocytic cell cultures provides novel insights into lineage-specific differentiation. *Experimental Hematology*, **35**, 476–489.
- Fuhrken, P.G., Apostolidis, P.A., Lindsey, S., Miller, W.M. & Papoutsakis, E.T. (2008a) Tumor suppressor protein p53 regulates megakaryocytic polyploidization and apoptosis. *Journal of Biological Chemistry*, **283**, 15589–15600.
- Fuhrken, P.G., Chen, C., Apostolidis, P.A., Wang, M., Miller, W.M. & Papoutsakis, E.T. (2008b) Gene Ontology-driven transcriptional analysis of CD34+ cell-initiated megakaryocytic cultures identifies new transcriptional regulators of megakaryopoiesis. *Physiological Genomics*, **33**, 159–169.
- Giammona, L.M., Fuhrken, P.G., Papoutsakis, E.T. & Miller, W.M. (2006) Nicotinamide (vitamin B3) increases the polyploidisation and proplatelet formation of cultured primary human megakaryocytes. *British Journal of Haematology*, **135**, 554–566.
- Herault, O., Colombat, P., Domenech, J., Degenne, M., Bremond, J.L., Sensebe, L., Bernard, M.C. & Binet, C. (1999) A rapid single-laser flow cytometric method for discrimination of early apoptotic cells in a heterogeneous cell population. *British Journal of Haematology*, **104**, 530–537.
- Hevehan, D.L., Papoutsakis, E.T. & Miller, W.M. (2000) Physiologically significant effects of pH and oxygen tension on granulopoiesis. *Experimental Hematology*, **28**, 267–275.
- Huang, Z., Dore, L.C., Li, Z., Orkin, S.H., Feng, G., Lin, S. & Crispino, J.D. (2009) GATA-2 reinforces megakaryocyte development in the absence of GATA-1. *Molecular and Cellular Biology*, **29**, 5168–5180.
- Ishiko, E., Matsumura, I., Ezoe, S., Gale, K., Ishiko, J., Satoh, Y., Tanaka, H., Shibayama, H., Mizuki, M., Era, T., Enver, T. & Kanakura, Y. (2005) Notch signals inhibit the development of erythroid/megakaryocytic cells by suppressing GATA-1 activity through the induction of HES1. *Journal of Biological Chemistry*, **280**, 4929–4939.
- Jirouskova, M., Shet, A.S. & Johnson, G.J. (2007) A guide to murine platelet structure, function, assays, and genetic alterations. *Journal of Thrombosis and Haemostasis*, **5**, 661–669.
- Jordan, K.C., Schaeffer, V., Fischer, K.A., Gray, E.E. & Ruohola-Baker, H. (2006) Notch signaling through tramtrack bypasses the mitosis promoting activity of the JNK pathway in the mitotic-to-endocycle transition of *Drosophila* follicle cells. *BMC Developmental Biology*, **6**, 16.
- Kang, B.H. & Altieri, D.C. (2006) Regulation of survivin stability by the aryl hydrocarbon receptor-interacting protein. *Journal of Biological Chemistry*, **281**, 24721–24727.
- Kawamura, T. & Yamashita, I. (2002) Aryl hydrocarbon receptor is required for prevention of blood clotting and for the development of vasculature and bone in the embryos of medaka fish, *Oryzias latipes*. *Zoological Science*, **19**, 309–319.
- Konieczna, I., Horvath, E., Wang, H., Lindsey, S., Saberwal, G., Bei, L., Huang, W., Platanias, L. & Eklund, E.A. (2008) Constitutive activation of SHP2 in mice cooperates with ICSBP deficiency to accelerate progression to acute myeloid leukemia. *Journal of Clinical Investigation*, **118**, 853–867.
- Lindsey, S., Zhu, C., Lu, Y.F. & Eklund, E.A. (2005) HoxA10 represses transcription of the gene encoding p67phox in phagocytic cells. *Journal of Immunology*, **175**, 5269–5279.
- Lindsey, S., Huang, W., Wang, H., Horvath, E., Zhu, C. & Eklund, E.A. (2007) Activation of SHP2 protein-tyrosine phosphatase increases HoxA10-induced repression of the genes encoding gp91(PHOX) and p67(PHOX). *Journal of Biological Chemistry*, **282**, 2237–2249.
- Ma, Q. & Whitlock, Jr, J.P. (1996) The aromatic hydrocarbon receptor modulates the Hepa 1c1c7 cell cycle and differentiated state independently of dioxin. *Molecular and Cellular Biology*, **16**, 2144–2150.
- Matsumura, I., Ishikawa, J., Nakajima, K., Oritani, K., Tomiyama, Y., Miyagawa, J., Kato, T., Miyazaki, H., Matsuzawa, Y. & Kanakura, Y. (1997) Thrombopoietin-induced differentiation of a human megakaryoblastic leukemia cell line, CMK, involves transcriptional activation of p21(WAF1/Cip1) by STAT5. *Molecular and Cellular Biology*, **17**, 2933–2943.
- McAdams, T.A., Miller, W.M. & Papoutsakis, E.T. (1998) pH is a potent modulator of erythroid differentiation. *British Journal of Haematology*, **103**, 317–325.
- Mercher, T., Cornejo, M.G., Sears, C., Kindler, T., Moore, S.A., Maillard, I., Pear, W.S., Aster, J.C. & Gilliland, D.G. (2008) Notch signaling specifies megakaryocyte development from hematopoietic stem cells. *Cell Stem Cell*, **3**, 314–326.
- Mercher, T., Raffel, G.D., Moore, S.A., Cornejo, M.G., Baudry-Bluteau, D., Cagnard, N., Jesneck, J.L., Pikman, Y., Cullen, D., Williams, I.R., Akashi, K., Shigematsu, H., Bourquin, J.P., Giovannini, M., Vainchenker, W., Levine, R.L., Lee, B.H., Bernard, O.A. & Gilliland, D.G. (2009) The OTT-MAL fusion oncogene activates RBPJ-mediated transcription and induces acute megakaryoblastic leukemia in a knockin mouse model. *Journal of Clinical Investigation*, **119**, 852–864.
- Miao, W., Hu, L., Scrivens, P.J. & Batist, G. (2005) Transcriptional regulation of NF-E2 p45-related

- factor (NRF2) expression by the aryl hydrocarbon receptor-xenobiotic response element signaling pathway: direct cross-talk between phase I and II drug-metabolizing enzymes. *Journal of Biological Chemistry*, **280**, 20340–20348.
- Michalek, J.E., Akhtar, F.Z., Longnecker, M.P. & Burton, J.E. (2001) Relation of serum 2,3,7,8-tetrachlorodibenzo-p-dioxin (TCDD) level to hematological examination results in veterans of Operation Ranch Hand. *Archives of Environmental Health*, **56**, 396–405.
- Miyazaki, R., Ogata, H. & Kobayashi, Y. (2001) Requirement of thrombopoietin-induced activation of ERK for megakaryocyte differentiation and of p38 for erythroid differentiation. *Annals of Hematology*, **80**, 284–291.
- Motohashi, H., Kimura, M., Fujita, R., Inoue, A., Pan, X., Takayama, M., Katsuoaka, F., Aburatani, H., Bresnick, E.H. & Yamamoto, M. (2010) NF-E2 domination over Nrf2 promotes ROS accumulation and megakaryocytic maturation. *Blood*, **115**, 677–686.
- Murata, K., Hattori, M., Hirai, N., Shinozuka, Y., Hirata, H., Kageyama, R., Sakai, T. & Minato, N. (2005) Hes1 directly controls cell proliferation through the transcriptional repression of p27Kip1. *Molecular and Cellular Biology*, **25**, 4262–4271.
- Nguyen, L.P. & Bradfield, C.A. (2008) The search for endogenous activators of the aryl hydrocarbon receptor. *Chemical Research in Toxicology*, **21**, 102–116.
- Pluim, H.J., Koppe, J.G., Olie, K., van der Slikke, J.W., Slot, P.C. & van Bostel, C.J. (1994) Clinical laboratory manifestations of exposure to background levels of dioxins in the perinatal period. *Acta Paediatrica*, **83**, 583–587.
- Quentmeier, H., Zaborski, M. & Drexler, H.G. (1998) Effects of thrombopoietin, interleukin-3 and the kinase inhibitor K-252a on growth and polyploidization of the megakaryocytic cell line M-07c. *Leukemia*, **12**, 1603–1611.
- Quintana, F.J., Basso, A.S., Iglesias, A.H., Korn, T., Farez, M.F., Bettelli, E., Caccamo, M., Oukka, M. & Weiner, H.L. (2008) Control of T(reg) and T(H)17 cell differentiation by the aryl hydrocarbon receptor. *Nature*, **453**, 65–71.
- Sakajiri, S., O'Kelly, J., Yin, D., Miller, C.W., Hofmann, W.K., Oshimi, K., Shih, L.Y., Kim, K.H., Sul, H.S., Jensen, C.H., Teisner, B., Kawamura, N. & Koeffler, H.P. (2005) Dlk1 in normal and abnormal hematopoiesis. *Leukemia*, **19**, 1404–1410.
- Schaeffer, V., Althausen, C., Shcherbata, H.R., Deng, W.M. & Ruohola-Baker, H. (2004) Notch-dependent Fizzy-related/Hec1/Cdh1 expression is required for the mitotic-to-endocycle transition in *Drosophila* follicle cells. *Current Biology*, **14**, 630–636.
- Schmidt, J.V., Su, G.H., Reddy, J.K., Simon, M.C. & Bradfield, C.A. (1996) Characterization of a murine Ahr null allele: involvement of the Ah receptor in hepatic growth and development. *Proceedings of the National Academy of Sciences of the United States of America*, **93**, 6731–6736.
- Shivdasani, R.A., Fujiwara, Y., McDevitt, M.A. & Orkin, S.H. (1997) A lineage-selective knockout establishes the critical role of transcription factor GATA-1 in megakaryocyte growth and platelet development. *EMBO Journal*, **16**, 3965–3973.
- Singh, K.P., Wyman, A., Casado, F.L., Garrett, R.W. & Gasiewicz, T.A. (2009) Treatment of mice with the Ah receptor agonist and human carcinogen dioxin results in altered numbers and function of hematopoietic stem cells. *Carcinogenesis*, **30**, 11–19.
- Stevens, E.A., Mezrich, J.D. & Bradfield, C.A. (2009) The aryl hydrocarbon receptor: a perspective on potential roles in the immune system. *Immunology*, **127**, 299–311.
- Thomsen, J.S., Kietz, S., Strom, A. & Gustafsson, J.A. (2004) HES-1, a novel target gene for the aryl hydrocarbon receptor. *Molecular Pharmacology*, **65**, 165–171.
- Tsai, F.Y. & Orkin, S.H. (1997) Transcription factor GATA-2 is required for proliferation/survival of early hematopoietic cells and mast cell formation, but not for erythroid and myeloid terminal differentiation. *Blood*, **89**, 3636–3643.
- Tsai, F.Y., Keller, G., Kuo, F.C., Weiss, M., Chen, J., Rosenblatt, M., Alt, F.W. & Orkin, S.H. (1994) An early haematopoietic defect in mice lacking the transcription factor GATA-2. *Nature*, **371**, 221–226.
- ten Tusscher, G.W., Steerenberg, P.A., van Loveren, H., Vos, J.G., von dem Borne, A.E., Westra, M., van der Slikke, J.W., Olie, K., Pluim, H.J. & Koppe, J.G. (2003) Persistent hematologic and immunologic disturbances in 8-year-old Dutch children associated with perinatal dioxin exposure. *Environmental Health Perspectives*, **111**, 1519–1523.
- Vannucchi, A.M., Bianchi, L., Cellai, C., Paoletti, F., Rana, R.A., Lorenzini, R., Migliaccio, G. & Migliaccio, A.R. (2002) Development of myelofibrosis in mice genetically impaired for GATA-1 expression (GATA-1(low) mice). *Blood*, **100**, 1123–1132.
- Vargiolu, M., Fusco, D., Kurelac, I., Dirnberger, D., Baumeister, R., Morra, I., Melcarne, A., Rimondini, R., Romeo, G. & Bonora, E. (2009) The tyrosine kinase receptor RET interacts in vivo with aryl hydrocarbon receptor-interacting protein to alter survivin availability. *Journal of Clinical Endocrinology and Metabolism*, **94**, 2571–2578.
- Walisser, J.A., Glover, E., Pande, K., Liss, A.L. & Bradfield, C.A. (2005) Aryl hydrocarbon receptor-dependent liver development and hepatotoxicity are mediated by different cell types. *Proceedings of the National Academy of Sciences of the United States of America*, **102**, 17858–17863.
- Wang, H., Lindsey, S., Konieczna, I., Bei, L., Horvath, E., Huang, W., Saberwal, G. & Eklund, E.A. (2009) Constitutively active SHP2 cooperates with HoxA10 overexpression to induce acute myeloid leukemia. *Journal of Biological Chemistry*, **284**, 2549–2567.
- Webb, K., Evans, R.G., Stehr, P. & Ayres, S.M. (1987) Pilot study on health effects of environmental 2,3,7,8-TCDD in Missouri. *American Journal of Industrial Medicine*, **11**, 685–691.
- Weissberg, J.B. & Zinkl, J.G. (1973) Effects of 2,3,7,8-tetrachlorodibenzo-p-dioxin upon hemostasis and hematologic function in the rat. *Environmental Health Perspectives*, **5**, 119–123.
- Yang, H., Miller, W.M. & Papoutsakis, E.T. (2002) Higher pH promotes megakaryocytic maturation and apoptosis. *Stem Cells*, **20**, 320–328.